

PRESENCE OF MULTIPLE STEADY STATES AND HYSTERESIS LOOP IN VISCOUS FLOWS

Gladys A. Zevallos- gzevallos@mec.puc-rio.br

Márcio da Silveira Carvalho – msc@mec.puc-rio.br

Department of Mechanical Engineering; Pontifícia Universidade Católica do Rio de Janeiro.
Rua Marquês de São Vicente, 225. Gávea. Rio de Janeiro, RJ, 22453-900, Brazil.

Abstract. Computational Fluid Dynamics has been used more and more to analize and optimize industrial processes. The flows that occur in these processes are non-linear and depend on different parameters. In order to obtain a complete understanding, a single steady state is not enough; information on how the flow states evolve as a given parameter varies is needed. Because of the non linearities, multiple steady states at the same set of parameters can and do occur, creating the possibility of hysteresis loops. The complete solution path can only be determined through continuation strategies that allow the computation of solutions around turning points. In this work, an Euler procedure, as a predictor step, and a pseudo-arc-length condition, as a corrector step, are used to construct the solution path of the flow inside a tilted lid driven cavity. The differential equations that govern the flow were discretized by the finite element / Galerkin's method, and the resulting set of non linear algebraic equations solved by Newton's method. The results show the presence of up to three different solutions at the same Reynolds number and a hysteresis loop.

Keywords: Hysteresis, Finite Element Method, Lid Driven Cavity.

1. INTRODUCTION

Theoretical predictions of steady states of laminar flows are obtained routinely by modern numerical techniques. Moreover, the development of commercial CFD software has spread the use of fluid flow analysis to optimize industrial processes. However, flows of practical interest depend on different parameters, and usually a single steady state is not enough for a complete understanding of the situation. An analysis on how the flow states evolve as the parameters vary is often necessary. An additional complication is that multiple solutions at a given set of parameters can and do occur, even in simple flow.

A robust and automatic approach has to be used to compute steady state solutions at different parameter values in order to be able to analyze the process flow in an efficient manner.

Because of the non-linearities present, each steady state solution has to be computed by some iterative method. For these methods to converge, a good initial guess has to be used at each parameter value. One approach largely employed is to use the solution at a previous parameter value as the initial guess for the next solution to be computed, what is known as a *zero-th order continuation*. This simple procedure may limit the variation of the changing parameter between two consecutive steady states. Moreover, solutions around turning points cannot be computed, limiting the ability of this strategy to analyze in an efficient way how the flow states evolve.

This work illustrates the use of Newton's method coupled with a predictor-corrector continuation strategy to automatically construct the entire solution path of a viscous flow. Newton's method was used to guarantee quadratic convergence close to the solution. In order to be able to compute solutions around turning points, and therefore predict hysteresis loops present in real process flows, the corrector step of the algorithm consisted of a pseudo-arc-length condition, as described by Bolstat and Keller (1986).

The results show that, at each parameter, steady state solution was obtained within 4 to 6 Newton's iteration. In the range of Reynolds number explored, two turning points were found, leading to a "S" shape path of solutions and a hysteresis loop. Up to three steady state solutions at the same Reynolds number were computed, two of them stable solutions that can be observed experimentally and one of them, unstable.

2. PROBLEM DEFINITION

The flow configuration used to test the solution and continuation strategy was the flow inside a tilted lid driven cavity, illustrated in Fig.1. The angle between the vertical and horizontal walls was fixed at $\alpha = 20^\circ$.

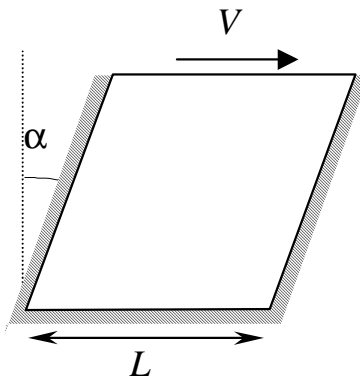


Figure 1: Sketch of tilted lid driven cavity.

This simple flow has important features of viscous flows like principal and secondary recirculations and has been largely used as test problems of different numerical techniques (see Ghia and Ghia, 1987). The flow inside the cavity is similar to the one inside a liquid pond of a

short dwell paper coater and its stability has been studied recently by Aidun et al. 1991 and Ramanan and Homsey 1994.

The goal was to analyze how the flow evolves as the Reynolds number rises, i.e. compute the solution path as function of the Reynolds number. The velocity and pressure field are governed by the momentum and continuity equations, which in dimensionless form are

$$\text{Re } \mathbf{v} \cdot \nabla \mathbf{v} - \nabla \cdot (-p\mathbf{I} + \nabla \mathbf{v} + \nabla \mathbf{v}^T) = 0 \quad \text{and} \quad \nabla \cdot \mathbf{v} = 0 \quad (1)$$

The Reynolds number is defined as $\text{Re} \equiv \rho VL / \mu$, where ρ is the liquid density, μ its viscosity, L is the cavity length and V is the lid velocity.

2.1 Solution Method

The differential equations that govern the problem were discretized by the finite element / Galerkin's method. Biquadratic basis functions ϕ_i were used for the velocity, and linear discontinuous functions ψ_i for the pressure. The domain was divided into 400 elements with 4562 degrees of freedom.

The weighted residuals of the Galerkin's method are:

$$\begin{aligned} R_{mx}^i &= \int_{\Omega} \left\{ \rho \phi_i \left(u \frac{\partial u}{\partial x} + v \frac{\partial u}{\partial y} \right) + \frac{\partial \phi_i}{\partial x} T_{xx} + \frac{\partial \phi_i}{\partial y} T_{xy} \right\} \|\mathbf{J}\| d\bar{\Omega} - \int_{\Gamma} \mathbf{e}_x \cdot (\mathbf{n} \cdot \mathbf{T}) \phi_i \frac{d\Gamma}{d\bar{\Gamma}} \\ R_{my}^i &= \int_{\Omega} \left\{ \rho \phi_i \left(u \frac{\partial v}{\partial x} + v \frac{\partial v}{\partial y} \right) + \frac{\partial \phi_i}{\partial x} T_{xy} + \frac{\partial \phi_i}{\partial y} T_{yy} \right\} \|\mathbf{J}\| d\bar{\Omega} - \int_{\Gamma} \mathbf{e}_y \cdot (\mathbf{n} \cdot \mathbf{T}) \phi_i \frac{d\Gamma}{d\bar{\Gamma}} \\ R_c^i &= \int_{\Omega} \left\{ \left(\frac{\partial u}{\partial x} + \frac{\partial v}{\partial y} \right) \psi_i \right\} \|\mathbf{J}\| d\bar{\Omega} \end{aligned}$$

Once the field variables are represented in terms of the basis functions, the system of partial differential equations become simultaneous algebraic equations for the coefficients of the basis functions.

$$\mathbf{R}(\mathbf{u}, \lambda) = 0 \quad (2)$$

In the system above, \mathbf{u} is the solution vector, and λ a parameter on which the problem depends. In the problem studied here, this parameter is the Reynolds number. This set of equations is non-linear due to the inertial term in the Navier-Stokes equation. The method of choice for this type of problem is Newton's method, which requires evaluation of the full Jacobian matrix, i.e.

$$\begin{aligned} \mathbf{J} \delta \mathbf{u} &= -\mathbf{R} \\ \mathbf{u}^{(k+1)} &= \mathbf{u}^{(k)} + \delta \mathbf{u} \end{aligned} \quad (3)$$

where \mathbf{J} is the Jacobian matrix of sensitivities of the residuals to the unknowns, i.e. $J_{ij} = \partial R_i / \partial u_j$. The iteration procedure (3) begins with an initial estimate $\mathbf{u}^{(0)}$ and continues until the system of equations (2) is nearly satisfied ($\|\mathbf{R}\| < 10^{-7}$). Because the basis functions used in the finite element method have compact support and vanish in most part of the domain, the Jacobian matrix is sparse. For this reason, all matrices were stored in compressed sparse formats, as described by Saad (1994). At each Newton iteration, the linear system of equation was solved using a multi-frontal solver, e.g. UMFPACK. Newton's method guarantees

quadratic convergence close to the solution. However, it can fail to converge if the initial guess is not close enough to the solution.

In order to start from a satisfactory initial approximation of the solution at each parameter value, some sort of continuation strategy has to be used. The simplest and the most common continuation strategy is what is known as the *zero-th order continuation*. The solution \mathbf{u}_0 , computed at a given parameter λ_0 is used as the initial guess for the iterative procedure used to compute the flow \mathbf{u}_1 at λ_1 , as illustrated in Fig.2. In order to have a satisfactory initial guess, the parameter step $\Delta\lambda = \lambda_1 - \lambda_0$ is limited to relative small values. This simple approach can be improved by using not only the solution \mathbf{u}_0 at λ_0 , but also its sensitivity $d\mathbf{u}/d\lambda$, to compute an initial guess $\mathbf{u}_1^{(0)}$ at λ_1 , as illustrate in Fig.2. This procedure is called a *first order continuation*:

$$\mathbf{u}_1^{(0)} = \mathbf{u}_0 + \frac{\partial \mathbf{u}}{\partial \lambda}(\lambda_1 - \lambda_0) \quad (4)$$

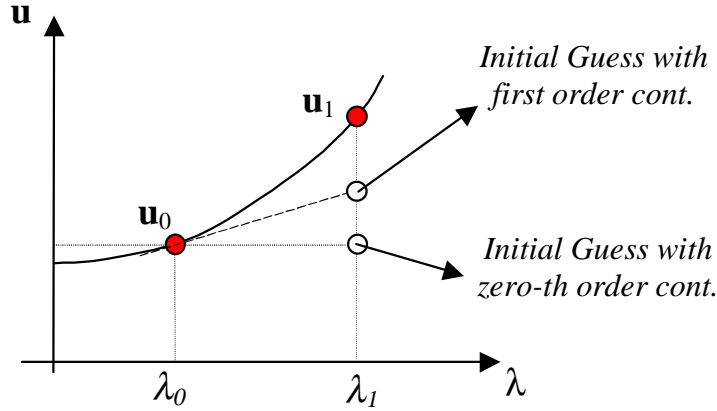


Figure 2: Geometric interpretation of Zero-th order and First order continuation.

The sensitivity of the solution with respect to the parameter λ can be evaluated with minimal computational cost:

$$\mathbf{J} \frac{\partial \mathbf{u}}{\partial \lambda} = - \frac{\partial \mathbf{R}}{\partial \lambda}$$

It is important to notice that at this point, the Jacobian matrix is already factorized and the computational cost of obtaining a much better initial guess with a first order continuation is simply the cost of a backward substitution. The information contained in the Jacobian matrix made first order continuation a natural choice. This is another important advantage of Newton's method.

An important limitation of first order continuation is that the procedure fails where the path of solutions in the parameter space has a turning point. A pseudo-arc-length continuation was used in this work together with the Newton's method, as described by Bolstad and Keller (1986), in order to overcome this problem.

2.2 Pseudo-Arc-Length Continuation

In this approach, the solution \mathbf{u} is not parameterized by the natural parameter λ , but instead by a pseudo-arc-length parameter s , as shown in Fig.3. This procedure requires an additional equation that relates the arc-length parameter to the solution \mathbf{u} and the natural parameter λ . The augmented system of equation is

$$\begin{aligned}\mathbf{R}(\mathbf{u}(s), \lambda(s)) &= 0 \\ N(\mathbf{u}(s), \lambda(s), s) &= 0\end{aligned}\quad (5)$$

There are several options for the normalization equation $N = 0$. In this work a linearization of the arc-length condition was used:

$$N(\mathbf{u}, \lambda, s) = \frac{d\mathbf{u}_0}{ds} \cdot (\mathbf{u}(s) - \mathbf{u}(s_0)) + \frac{d\lambda_0}{ds} (\lambda(s) - \lambda(s_0)) - (s - s_0) = 0 \quad (6)$$

The augmented system was solved by Newton's method, with initial guess obtained from a first-order continuation (predictor step). Figure 3 illustrates the iterative procedure described next.

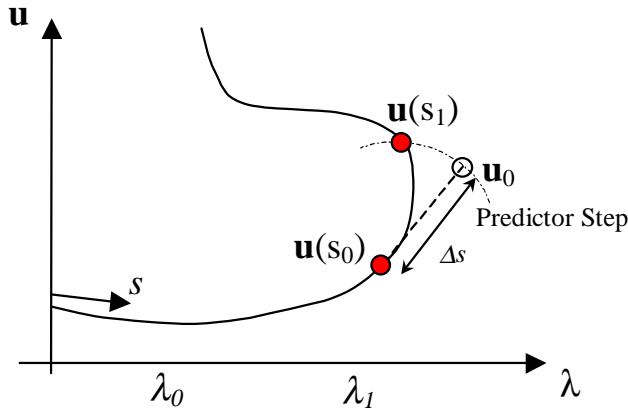


Figure 3: Sketch of the pseudo arc length continuation procedure.

Predictor Step. The predictor step consist of a first order continuation on the arc-length parameter; as shown by the following expressions.

$$\begin{aligned}\mathbf{J} \frac{\partial \mathbf{u}}{\partial \lambda} &= - \frac{\partial \mathbf{R}}{\partial \lambda} \\ \frac{\partial \lambda}{\partial s} &= \pm \left[1 + \left\| \frac{\partial \mathbf{u}}{\partial \lambda} \right\|^2 \right]^{-1/2} \\ \frac{\partial \mathbf{u}}{\partial s} &= \frac{\partial \lambda}{\partial s} \frac{\partial \mathbf{u}}{\partial \lambda}\end{aligned}$$

$$\mathbf{u}^{(0)} = \mathbf{u}_0 + \frac{\partial \mathbf{u}}{\partial s} \Delta s$$

$$\lambda^{(0)} = \lambda_0 + \frac{\partial \lambda}{\partial s} \Delta s$$

Corrector Step. Once an initial guess is obtained, the augmented system (5) is solved by Newton's method.

$$\begin{bmatrix} \mathbf{J} & \frac{\partial \mathbf{R}}{\partial \lambda} \\ \frac{\partial N}{\partial \mathbf{u}} & \frac{\partial N}{\partial \lambda} \end{bmatrix} \begin{bmatrix} \delta \mathbf{u} \\ \delta \lambda \end{bmatrix} = - \begin{bmatrix} \mathbf{R} \\ N \end{bmatrix}$$

Since the Jacobian matrix is sparse and banded and the augmented system is not, a bordering algorithm was used in order to take advantage of the structure of the Jacobian matrix. The solution procedure is:

$$\mathbf{J} \mathbf{a} = \frac{\partial \mathbf{R}}{\partial \lambda}$$

$$\mathbf{J} \mathbf{b} = -\mathbf{R}$$

$$\delta \lambda = \frac{\left(N + \left(\frac{\partial N}{\partial \mathbf{u}} \right)^T \mathbf{b} \right)}{\left(\frac{\partial N}{\partial \lambda} - \left(\frac{\partial N}{\partial \mathbf{u}} \right)^T \mathbf{a} \right)}$$

$$\delta \mathbf{u} = \mathbf{b} - \delta \lambda \mathbf{a}$$

3. RESULTS

The continuation procedure described in the previous section was used to construct the path of steady state solutions of the flow inside a tilted lid driven cavity as a function of the Reynolds number. The path started at vanishing Reynolds number. In this case, the problem is linear and Newton's method converges in one iteration. Each steady state solution converged within up to 8 Newton's iteration and took about 6 minutes to be computed in a Pentium III 450 MHz computer.

Figure 4 illustrates the solution path. It shows how the L_2 norm of the solution vector varies with the Reynolds Number. The streamlines of selected states are shown in Fig.5. In the range of Reynolds number explored, the solution path presented two turning points. It is important to notice that flow states c , e and f , shown in Fig.5, occur exactly at the same Reynolds number. They are multiple solutions of the same problem.

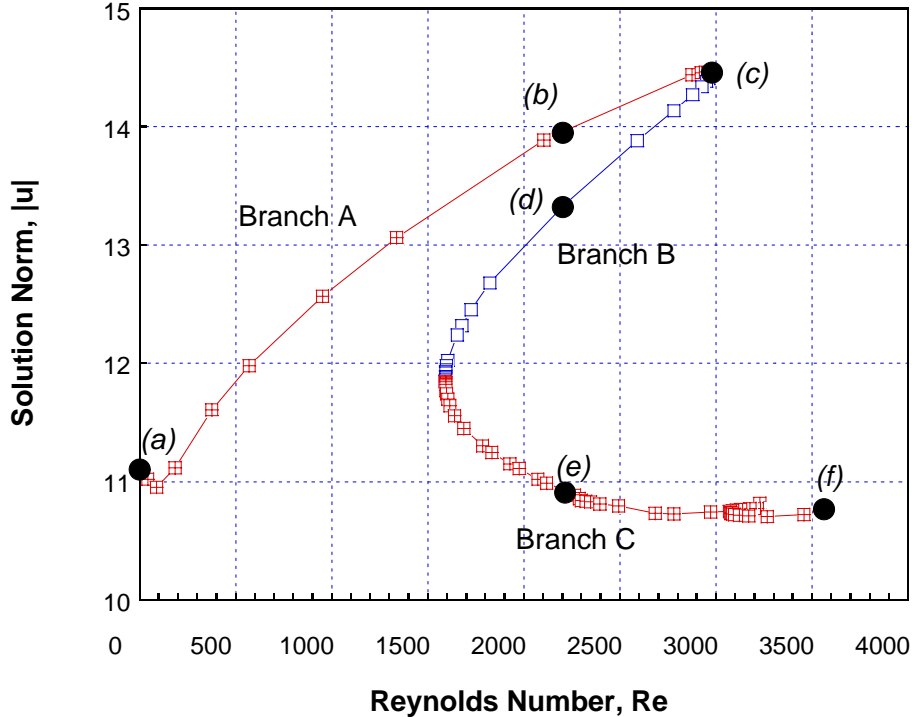


Figure 4: Solution path as a function of the Reynolds Number.

The stability of the flow was not investigated. Nevertheless, it is well established that the stability of solutions along a branch in the parameter space changes at a regular turning point (see Iooss and Joseph, 1980). The top and bottom branch in Fig.4 (branches A and C) are stable. Branch B, between turning points #1 and #2, is unstable. These flow states cannot be observed experimentally. Even small disturbances in the velocity and pressure field, that are always present in reality, would lead to another stable flow state.

Tracking the solution path along branch A in the direction of rising Reynolds number, shows that the recirculation inside the cavity becomes smaller. A turning point occurs at $Re = 2973.8$. Above this value, the only steady state solution possible is along branch C. Experimentally, the flow would jump from flow states along branch A to flow states along branch C. The flow pattern changes dramatically when this transition occurs (compare flow states *c* at $Re = 2973.8$ and *f* at $Re = 3500$).

Because the solution path has an S shape, the flow analyzed here has an hysteresis effect. Flow state *f*, in branch C, cannot be achieved in the laboratory by raising the Reynolds number from zero. This behavior has been observed experimentally by Aidun et al. (1991) in the flow inside a short dwell paper coater.

In order to compare the procedure described here with the capability of commercial CFD programs, that, to the best of the authors' knowledge, rely on zero-th order continuation, the flow inside a tilted lid driven cavity was solved using the software Fluent, by Fluent Inc. Because all the variables were not solved simultaneously in the iterative procedure used by this particular program, the radius of convergence was much larger than the radius of convergence of Newton's method. Solutions could be obtained even with poor initial guesses. However, the number of iterations and computational cost (time) were much larger than the number of iterations and cost of Newton's method. Solutions were obtained up to $Re = 3500$. The

solution paths constructed following the direction of rising and falling Reynolds number were exactly the same. A continuation strategy based on zero-th order continuation could not predict multiple solutions nor the presence of a hysteresis loop in the flow.

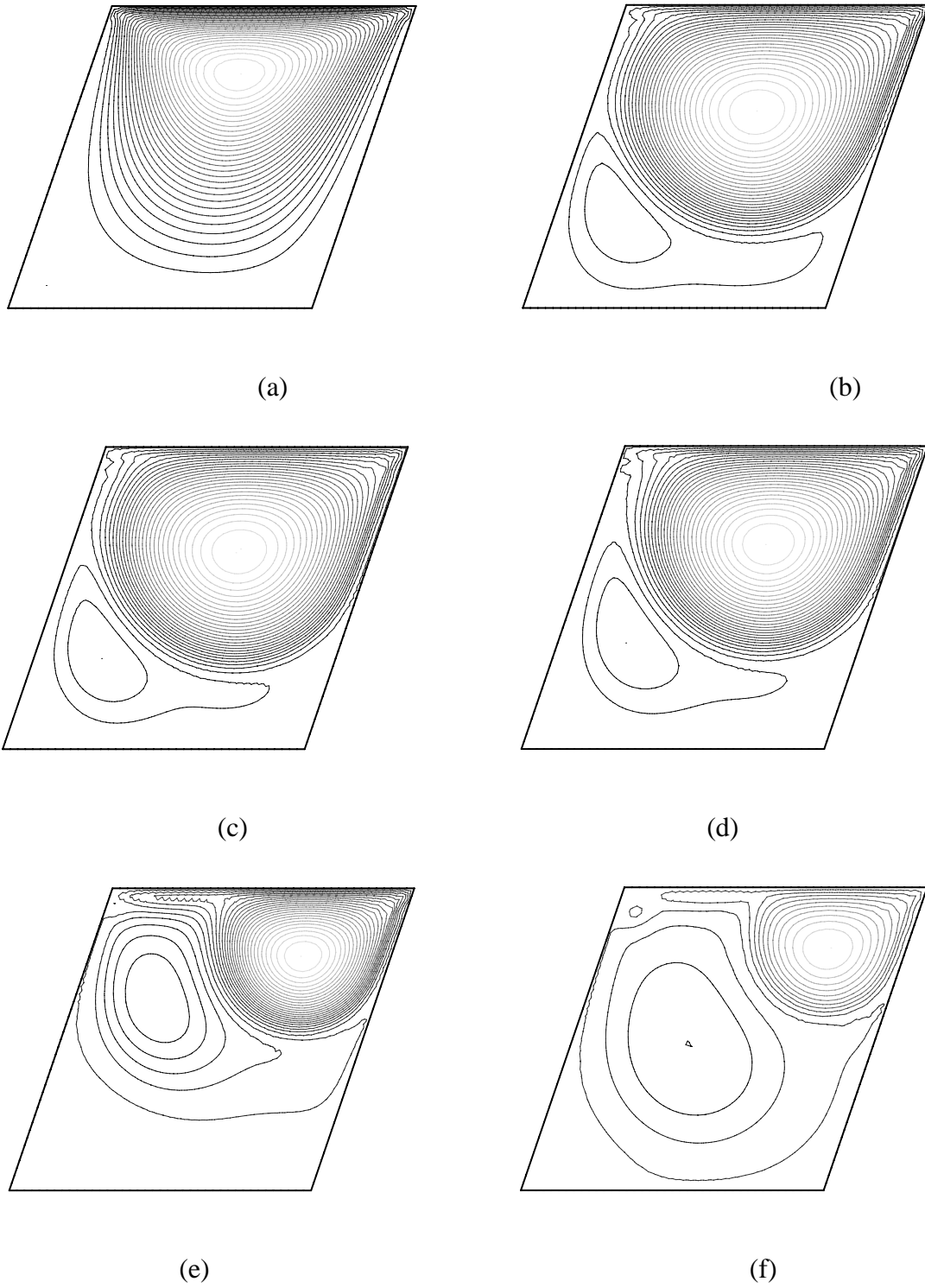


Figure 5: Streamlines of selected flow states. Flow states *c*, *e* and *f* are multiple solutions of the problem. They occur at the same Reynolds Number.

4. FINAL REMARKS

Computational Fluid Dynamics reached a stage at which solutions of steady, two-dimensional laminar flows can be routinely obtained. However, in order to use this capability to understand and optimize industrial processes, it is necessary to predict how flow states vary with different operating parameters.

Newton's method coupled with a pseudo-arc-length continuation strategy was used to automatically construct the entire path of steady states of the flow inside a tilted lid driven cavity. Even this simple flow presented a complicated behavior, with turning points, multiple solutions and hysteresis loop. This type of behavior has been observed experimentally in many important industrial flow processes.

A procedure based on zero-th order continuation was also tested and was not capable of predicting this type of behavior. This limitation can hide important features of the flow being analyzed and compromise the full understanding of the situation.

Acknowledgements

G. A. Zevallos is sponsored by a scholarship from CAPES.

REFERENCES

- Aidun, C. K., Triantafillopoulos, N. G. & Benson, J. D., 1991, Global Stability of lid-driven cavity with throughflow: Flow visualization studies, Physics of Fluids, vol. 3, pp.2081.
- Bolstad, J. H. & Keller, H. B., 1986, A multigrid continuation method for elliptic problems with folds, SIAM J. Sci. Stat. Comput., vol.7(4), pp.1081.
- Ghia, U., Ghia, K. N. & Shin, C. T., 1987, High Re solutions for incompressible flows using Navier-Stokes equations and a multi-grid method, Journal of Computational Physics, vol.48, pp.387.
- Keller, H. B., 1977, Numerical Solution of Bifurcation and Nonlinear Eigenvalue Problem, in Applications of Bifurcation Theory (ed. P. H. Rabinowitz), Academic Press.
- Ramanan, N. & Homsy, G. M., 1994, Linear Stability of Lid Driven Cavity Flows, Physics of Fluids, vol.6(8), pp.2690.